Quasiatomic contributions to molecular-scattering form factors

M. Cavagnero*
Department of Physics and Astronomy, The University of Nebraska–Lincoln, Lincoln, Nebraska 68588-0111
(Received 4 August 1989)

The scattering form factors for excitation of H_2^+ in fast collisions are calculated in a sequence of approximations revealing their dependence on details of the initial- and final-state wave functions. Each approximate calculation is compared directly to the "exact" results obtained with separable, fixed-nuclei wave functions. Even for interproton separations larger than those for which the united-atom limit applies, the quasiatomic character of the final-state orbital dominates transition amplitudes to low-lying dissociative states. Possible applications to molecular dissociation by charged-particle impact at high energies are considered.

I. INTRODUCTION

The interpretation of electron-molecule collision experiments is often hindered by the complexity of existing methods of evaluating wave functions of electrons moving in anisotropic molecular fields. It is generally recognized, however, that the highest-occupied and lowest-unoccupied molecular orbitals, which dominate low-energy electron-molecule and atom-molecule collisions, often resemble simple atomic orbitals and can be approximated by superimposing a few spherical waves centered on the molecular center of mass. The purpose of this article is to demonstrate that the quasiatomic character of these molecular orbitals determines their excitation amplitudes in high-energy processes, such as dissociation by collision with fast charged particles.

This work may be regarded as an extension of the remarks by Dunn,[1] who noted that angular distributions of dissociation products in fast collisions reflect the dependence of the scattering amplitudes on the orientation $\hat{\mathbf{K}}\cdot\hat{\mathbf{R}}=\cos\theta$ of the momentum transfer $\mathbf{K}$ relative to an axis of the molecule $\mathbf{R}$. Dunn used symmetry arguments to determine which molecular orbitals had nonvanishing amplitudes for parallel ($\theta=0$) and perpendicular ($\theta=\pi/2$) molecular orientations. Here, the entire K and θ distributions of the "exact" scattering amplitudes are examined and then quantitatively reproduced using a suitably scaled Coulomb wave function for the final-state orbital. The calculations are performed for H_2^+, since it is the only system for which comparison with exact results is possible. The calculation of the "exact" H_2^+ form factors was outlined earlier by Peek[2] (for discrete) and by Kimura[3] (for continuum transitions).

In Sec. II A, I briefly review the approximations used in calculating amplitudes for the process

$$e^- + H_2^+(1s\sigma) \rightarrow H_2^+(N) + e^- \searrow H(nlm) + p^+ \,. \quad (1)$$

Following Peek,[4] I assume that the molecular-ion states are correctly represented by Born-Oppenheimer (fixed-nuclei) wave functions and that the electronic excitation in process (1) is fast compared to molecular vibrations and rotations. The scattering amplitudes at fixed interproton separation R are then calculated in first Born approximation. These are the so-called "exact" results to which all subsequent calculations will be compared.

In Sec. II B, the $\mathbf{K}$ dependence of the "exact" scattering amplitudes for each of the low-lying dissociative states is shown to vary slowly with interproton separation. In particular, the *qualitative* $\mathbf{K}$ dependence of the form factors is the same at the united-atom limit ($R=0$) as at the equilibrium ground-state separation ($R=2$ a.u.). In part, this reflects the symmetry arguments of Ref. 1, which hold at any internuclear separation, R. It also reflects the adiabatic R dependence of both the initial- and final-state orbitals.

Section III presents scattering form factors obtained in a sequence of approximations based on a quasiatomic model of the molecular orbitals. Some of the R dependence of the form factors is incorporated in Sec. III A by replacing the united-atom limit wave functions with scaled Coulomb wave functions, where the scaling parameters are adjusted at each R to correctly represent the initial- and final-state binding energies. Most of the remaining features of the form factors are then accounted for in Sec. III B, where the scaled Coulomb approximation is retained for the final state, but the initial state is accurately represented. The concentration of the ground $1s\sigma$ state electron density at the protons is seen to be essential for quantitative predictions. Angle-averaged scattering probabilities are presented in Sec. III C to facilitate quantitative comparisons. This is followed by a brief discussion and summary in Sec. IV.

II. SCATTERING FORM FACTORS

A. Born approximation

Peek[4,5] has expressed Born's approximation to the total cross section for excitation of the Nth electronic state of H_2^+ in terms of a fixed-nuclei cross section $Q_N(R)$ averaged over the nuclear probability distribution in the initial vibrational state v

$$Q_{Nv}=\int_0^\infty R^2 dR\,|F_v(R)|^2 Q_N(R)\ . \tag{2}$$

The fixed-nuclei cross section is given by the square of a scattering amplitude averaged over the magnitude and direction of the momentum transfer $\mathbf{K}$,

$$Q_N(R)=2\pi\left[\frac{2}{V_{\rm inc}^2}\right]\times\int_{k_0-k_N}^{k_0+k_N}\frac{dK}{K^3}\int_0^\pi \sin\theta\, d\theta\,|\varepsilon_N(R,K,\theta)|^2\ . \tag{3}$$

Here, θ is the angle between $\hat{\mathbf{K}}$ and the interproton axis $\hat{\mathbf{R}}$; the azimuthal angle about $\hat{\mathbf{K}}$ has been integrated to obtain the factor of 2π, and the limits of integration over K are fixed by momentum conservation. All quantities are expressed in atomic units.

The basic parameters determining the cross section are thus the scattering form factors

$$\varepsilon_N(R,K,\theta)=\int d\mathbf{r}\,\Psi_N^*(R;\mathbf{r})e^{i\mathbf{K}\cdot\mathbf{r}}\Psi_{1s\sigma}(R;\mathbf{r})\ , \tag{4}$$

where the $\Psi(R;\mathbf{r})$ are Born-Oppenheimer adiabatic wave functions of the molecular ion, defined with respect to the quantization axis $\hat{\mathbf{R}}$. Within the range of validity of Born's approximation, the form factors ε_N are also the basic parameters for the calculation of generalized oscillator strengths,[6] angular distributions of the dissociation fragments,[7] and other observables. The subsequent discussion will accordingly be restricted to an analysis of the R, K, and θ dependence of ε_N for various electronic states N. I will focus on small-N final states, since these have the greatest amplitude in the vicinity of the ground $1s\sigma$ orbital.

B. R dependence of the form factors

The contribution to the total scattering cross section Eq. (2) from collisions at small interproton separations R is readily determined by using orbitals of the united-atom limit (He^+) in Eq. (4). In this limit, the dependence of the scattering form factors on θ is simply

$$\lim_{R\to 0}\varepsilon_N=\varepsilon_{nlm}(K,\theta)=i^l\sqrt{2l+1}(n,l|j_l(Kr)|1s)d^l_{0m}(\theta)\ , \tag{5}$$

where d is a rotation function and $(n,l|j_l(Kr)|1s)$ is the radial integral

$$(n,l|j_l(Kr)|1s)=\int_0^\infty r^2 dr\,R_{nl}(r)j_l(Kr)R_{1s}(r)\ . \tag{6}$$

The inelastic component of the scattered wave is then

$$\lim_{R\to 0}\Psi_{ie}^{\rm Sc}\propto\sum_n\frac{e^{ik_n r}}{r}\sum_l i^l\sqrt{2l+1}(n,l|j_l(Kr)|1s)\times\sum_m d^l_{0m}(\theta)\Psi_{nlm}(\mathbf{r})=\sum_n\frac{e^{ik_n r}}{r}\sum_l i^l\sqrt{2l+1}(n,l|j_l(Kr)|1s)\Psi_{nl0}(\mathbf{r}') \tag{7}$$

indicating that the final state is aligned along the direction of the momentum transfer (that is, $l\cdot\mathbf{K}=0$) and is independent of the orientation of the internuclear axis $\hat{\mathbf{R}}$. [Note that $\mathbf{r}$ in Eq. (7) is defined with respect to the molecular axis, while $\mathbf{r}'$ is defined with respect to $\hat{\mathbf{K}}$.]

For $R>0$ the integrals in Eq. (4) cannot be evaluated analytically. However, due to the separability of the Born-Oppenheimer wave functions in prolate spheroidal coordinates,[8] Eq. (4) can be reduced to a sum of one-dimensional integrals.[2] We have evaluated these integrals numerically by 28-point Gauss-Laguerre quadrature.

The K and θ dependence in the united-atom limit, given by Eq. (5), is shown in Figs. 1(a)–3(a) for the $2p\sigma(m=0)$, $2p\pi(m=1)$, and $3d\sigma(m=0)$ final states, re-

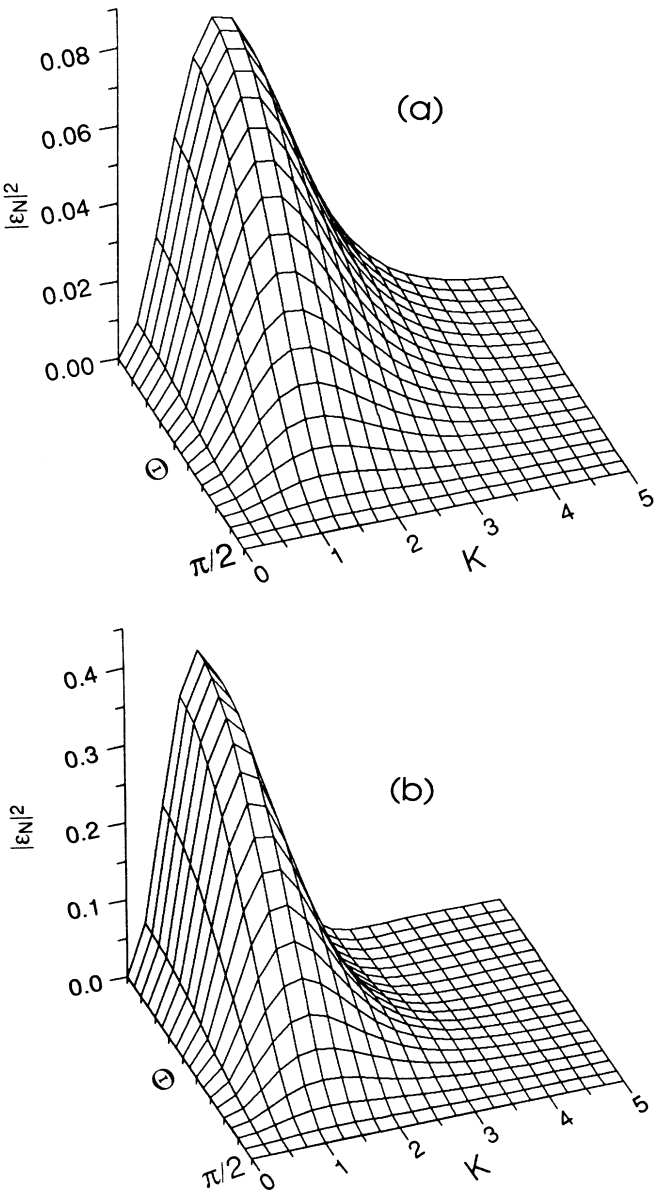

FIG. 1. The exact θ and K dependence of the scattering probability $|\varepsilon_N|^2$ for the $1s\sigma\to 2p\sigma$ transition (a) in the united-atom limit $R=0$; and (b) at $R=2$ a.u.

spectively. (Note that $|\varepsilon_N|^2$ has been plotted for comparison with other references.) The θ dependence of these plots is simply $\cos^2\theta$, $\sin^2\theta$, and $(3\cos^2\theta-1)^2$, respectively.

Also shown in Figs. 1(b)–3(b) is the K and θ dependence of the exact form factors, Eq. (4), at an interproton separation of $R=2$ a.u. Strikingly, the shapes of the exact form factors at $R=2$ (the approximate minimum of the $1s\sigma$ potential well) closely resemble those of the united-atom limit. In particular, the maxima and minima of ε_N, and the number of its nodes, are governed by symmetry considerations and are insensitive to variations in R.[1]

Several elementary conclusions can be drawn from this comparison. Note first that the contribution to $Q_N(R)$ from the θ integral in Eq. (3) is independent of m in the united-atom limit, since

$$\int_0^{\pi}\sin\theta\, d\theta |d^l_{0m}(\theta)|^2=\frac{2}{2l+1}\ . \tag{8}$$

Thus, near $R=0$, the $2p\sigma$ and (two) $2p\pi$ orbitals give comparable contributions to $Q_N(R)$.

As R increases, the form factor for $2p\sigma$ excitation increases much faster than that for $2p\pi$ excitation. That the magnitude of the π amplitude is less sensitive to variations in R than is the σ amplitude, reflects the fact that the π orbital has a node along the interproton axis, where the $1s\sigma$ orbital peaks. At $R=2$, the $2p\sigma$ cross section (averaged over $\sin\theta\, d\theta$) is already twice that of the $2p\pi$ state. However, since there are two $2p\pi$ orbitals, the production of $2p\pi$ states remains comparable to the $2p\sigma$ excitation out to the minimum of the ground-state potential curve.[9]

Since transitions at small internuclear separations ($R\leq 2$) yield dissociation fragments with large relative velocities, we conclude that $2p\sigma$ and $2p\pi$ orbitals yield comparable contributions to the production of fast fragments. (The same could be said for the relative population of m states of higher nl manifolds.) Furthermore, the $2p\pi$ orbitals dissociate to $2p$ states of atomic hydrogen, so that substantial Lyman-α radiation will accom-

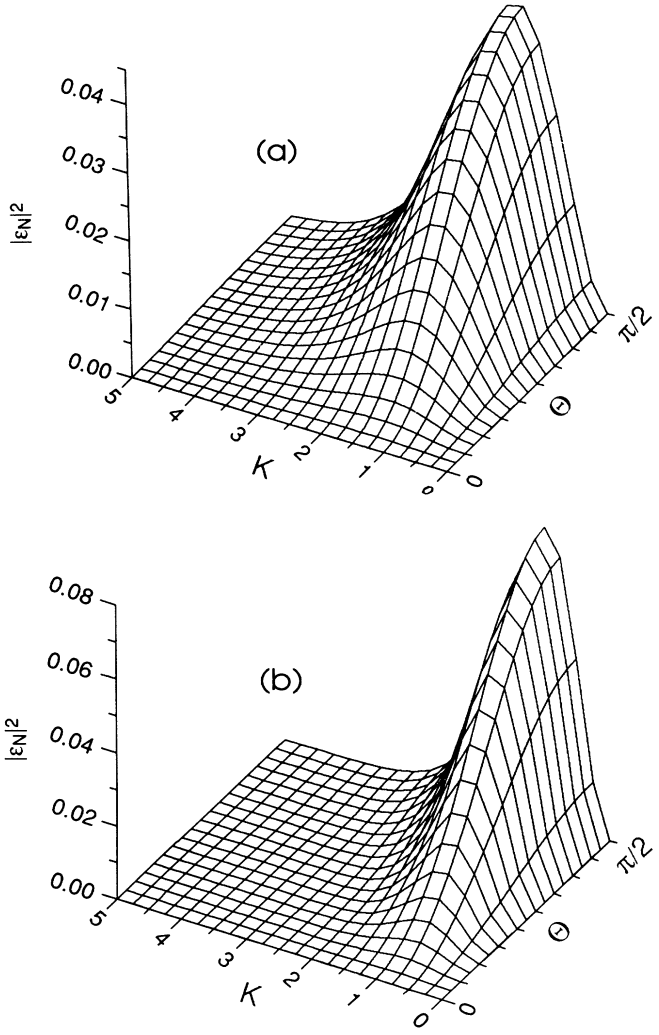

FIG. 2. The same as Fig. 1 for the $1s\sigma\rightarrow 2p\pi$ transition.

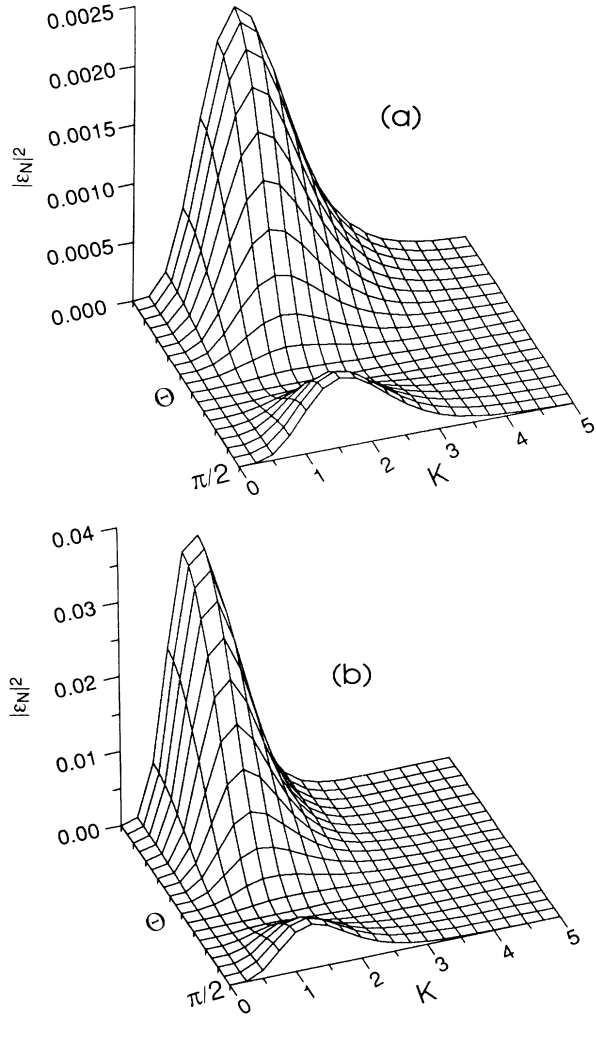

FIG. 3. The same as Fig. 1 for the $1s\sigma\rightarrow 3d\sigma$ transition.

pany the fast fragments, a result similar to that obtained in slow H_2^+-He collisions.[10]

III. THE QUASIATOMIC MODEL

A. Scaled atomic-orbital approximation

As mentioned above, the magnitudes of the form factors in Figs. 1–3 vary considerably with interproton separation. This variation results, in part, from the R dependence of the binding energy of the initial- and final-state electronic orbitals. This is illustrated in Fig. 4, where I have simply replaced the He^+ wave functions used above, by scaled Coulomb wave functions with binding energies (or effective charges) determined by the $R=2$ values of the exact H_2^+ potential curves.[8]

Note that the squared form factor for $2p\pi$ excitation, Fig. 4(b), is now nearly equal in magnitude to the exact result in Fig. 2(b). Scaling likewise enhances the $2p\sigma$ and $3d\sigma$ form factors in Figs. 4(a) and 4(c), though these remain somewhat smaller than their exact values in Figs. 1(b) and 3(b), respectively. The remaining discrepancy in the magnitudes of the σ form factors is due primarily to higher multipole components of the ground $1s\sigma$ state, as will be demonstrated in Sec. III B.

Another qualitative feature apparent in Figs. 1–3 is that as R increases, the transition amplitudes shift to smaller values of the momentum transfer. This shift results primarily from the increasing spatial extent (or decreasing binding energy) of the $1s\sigma$ orbital as the inter-

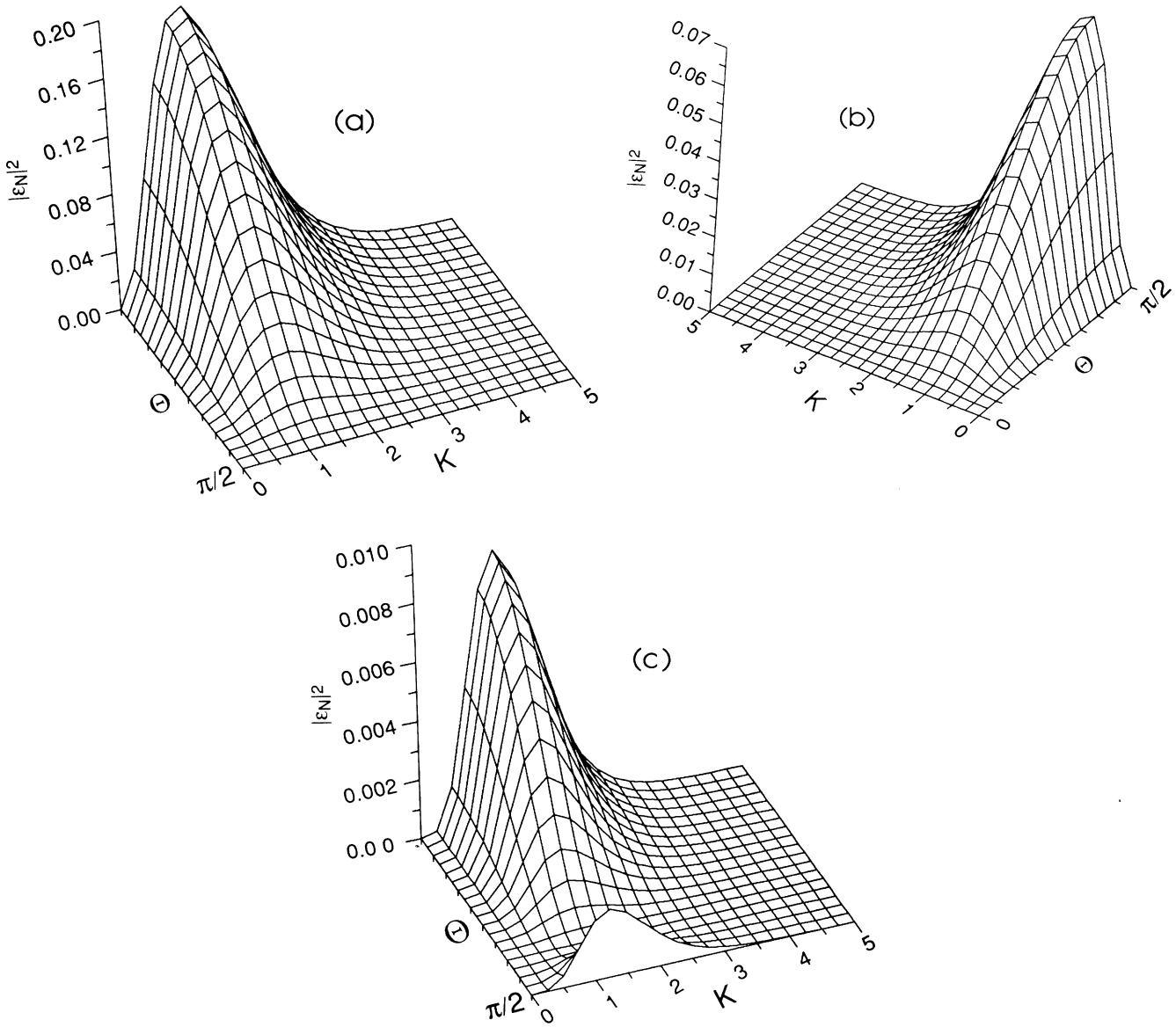

FIG. 4. The θ and K dependence of the scattering probability at $R=2$ a.u. using scaled Coulomb wave functions for both the initial ($1s\sigma$) and the final states: (a) $2p\sigma$, (b) $2p\pi$, and (c) $3d\sigma$.

proton separation increases. (The binding energies of the final-state orbitals can either increase or decrease with R, but generally vary over a much smaller range than the $1s\sigma$ binding energy.) The shift is important because the $1/K^3$ factor in the cross section, Eq. (3), heavily weights contributions from small K (see Sec. III C). A shift toward smaller values of K is indeed apparent in comparing Fig. 4 with Figs. 1(a)–3(a). However, in the scaled atomic-orbital approximation, the shift is independent of θ, a shortcoming addressed in the next section.

B. Exact initial-, scaled final-state approximation

As mentioned above, the peaking of the $1s\sigma$ wave function at the nuclear centers considerably enhances the excitation amplitudes for σ states. Furthermore, the shift of the scattering amplitudes toward smaller values of K as R increases was approximated in the preceding section without regard to the relative orientation of $\mathbf{K}$ and the initial $1s\sigma$ state. In fact, as R increases, the range of the $1s\sigma$ orbital increases primarily along $\hat{\mathbf{R}}$, and accordingly, the K shift should be most pronounced along $\theta=0$ and should be small near $\theta=\pi/2$. While the K distributions in Figs. 4(a) and 4(c) peak at smaller-K values than the united-atom limit distributions in Figs. 1(a) and 3(a), the exact distributions in Figs. 1(b) and 3(b) show even more pronounced shifts near $\theta=0$.

To demonstrate that these shortcomings stem from improper representation of the initial state, I have recalculated the form factors using the exact $1s\sigma$ wave function, but retaining scaled Coulomb wave functions for the final states. The results are shown in Fig. 5 for the $2p\sigma$ and $2p\pi$ excitations. These compare quite favorably, both in magnitude and in shape, with the exact results presented above. Note that the form factors vanish at $K=0$, since orthogonality to the $1s\sigma$ orbital is guaranteed by symmetry in this case.

For the $3d\sigma$ excitation, the scaled Coulomb final state is not orthogonal to the exact $1s\sigma$ orbital at $R=2$ a.u. This results in a spurious contribution to the form factor, which is significant for small momentum transfers. A reasonable comparison can still be made, however, by orthogonalizing the final state to the exact $1s\sigma$ wave function, i.e., by representing the $3d\sigma$ wave function in the form

$$\Psi'=\frac{1}{(1+S^2)^{1/2}}(\Psi_{\text{atomic}}-S\Psi_{1s\sigma}) , \tag{9}$$

where S is the overlap integral $\langle\Psi_{1s\sigma}|\Psi_{\text{atomic}}\rangle$. The result is shown in Fig. 6. The overall shape of the resultant form factor, including the K shift described above, is now quite comparable to the exact result shown in Fig. 3(b).

As a further illustration of the quasiatomic nature of the final-state wave functions, the K and θ dependence of the $1s\sigma$-$2s\sigma$ transition at $R=2$ a.u. is plotted in Fig. 7.

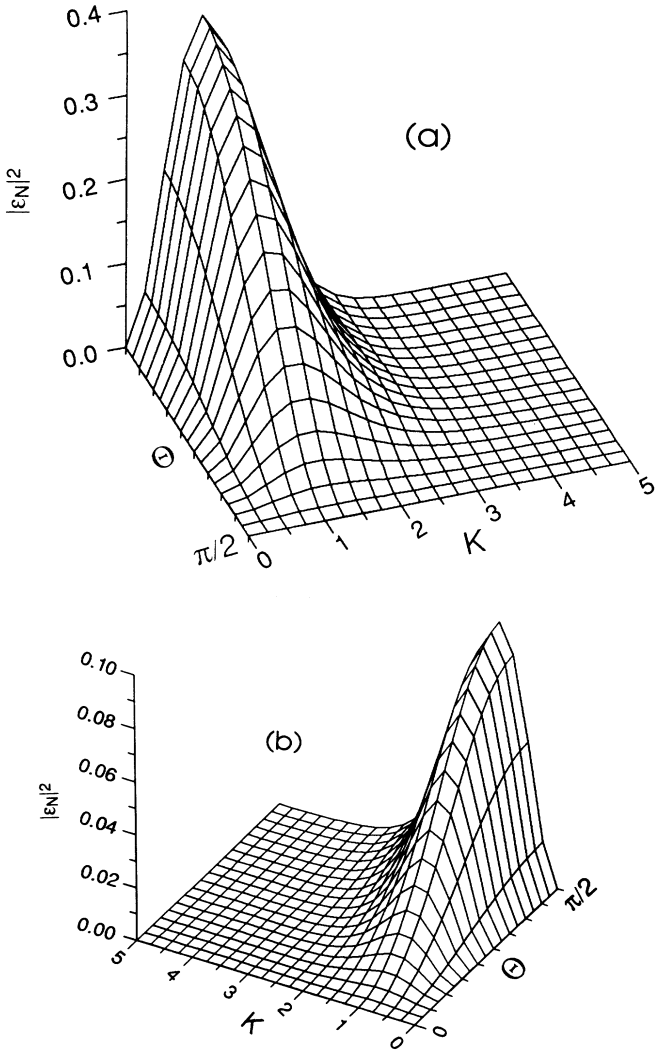

FIG. 5. The θ and K dependence of the scattering probability at $R=2$ a.u. using the exact $1s\sigma$ wave function and scaled Coulomb wave functions for the (a) $2p\sigma$ and (b) $2p\pi$ final states.

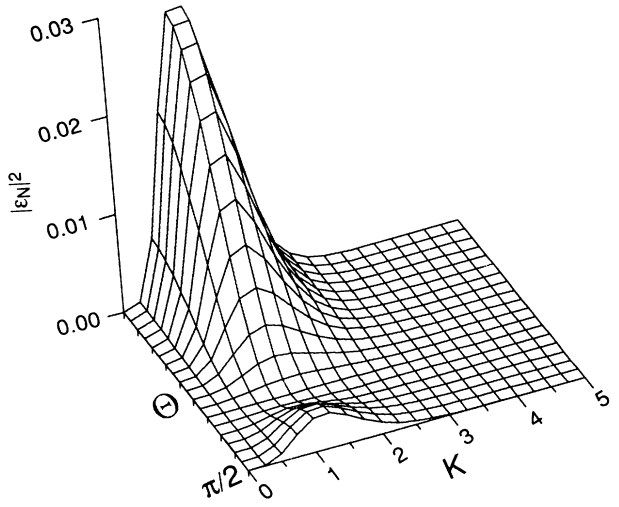

FIG. 6. The same as Fig. 5 for the $3d\sigma$ final state. The scaled Coulomb $3d\sigma$ orbital has been orthogonalized to the ground state, as in Eq. (9).

Figure 7(a) is the exact result, while Fig. 7(b) was obtained using a scaled Coulomb final state [orthogonalized to the ground state, as in Eq. (9)]. Clearly, this form factor is nearly independent of θ over a wide range of K. Note that $|\varepsilon_N|^2/K^2$ is plotted versus $\ln(K^2)$ in these figures, as in Sec. III C, to emphasize the contribution to the cross section, Eq. (3), from small momentum transfers.

C. Quantitative comparisons

The $3d$ illustrations in the previous sections reveal the full K and θ distributions of the form factors, but are not easily used for quantitative comparison. Accordingly, I present here a few results of θ-averaged probabilities, which enter Eq. (3). Defining[3]

$$|\varepsilon_N(R,K)|^2=\tfrac{1}{2}\int_0^{\pi}\sin\theta\, d\theta\,|\varepsilon_N(R,K,\theta)|^2 , \tag{10}$$

Eq. (3) can be written

$$Q_N(R)=2\pi\left[\frac{2}{V_{\rm inc}^2}\right]\int_{\ln k_{\rm min}^2}^{\ln k_{\rm max}^2} d(\ln K^2)\frac{|\varepsilon_N(R,K)|^2}{K^2} , \tag{11}$$

where $k_{\rm min}=k_0-k_N$ and $k_{\rm max}=k_0+k_N$.

The integrand in Eq. (11) is plotted as a function of $\ln K^2$ in Figs. 8(a) and 8(b) for the $2p\sigma$ and $2p\pi$ excitations, respectively. The shape and magnitude of the results obtained using scaled Coulomb final states (dashed curves) are again quite comparable to the exact values (solid curves). Differences of roughly 5–10 % remain in the optical limit, $K\to 0$. I emphasize, however, that these remaining differences need not reflect contributions from higher partial waves in the final states, since I have not attempted to optimize the radial parts of the scaled Coulomb wave functions. Use of a formally exact single-center expansion is beyond the scope of this preliminary investigation.

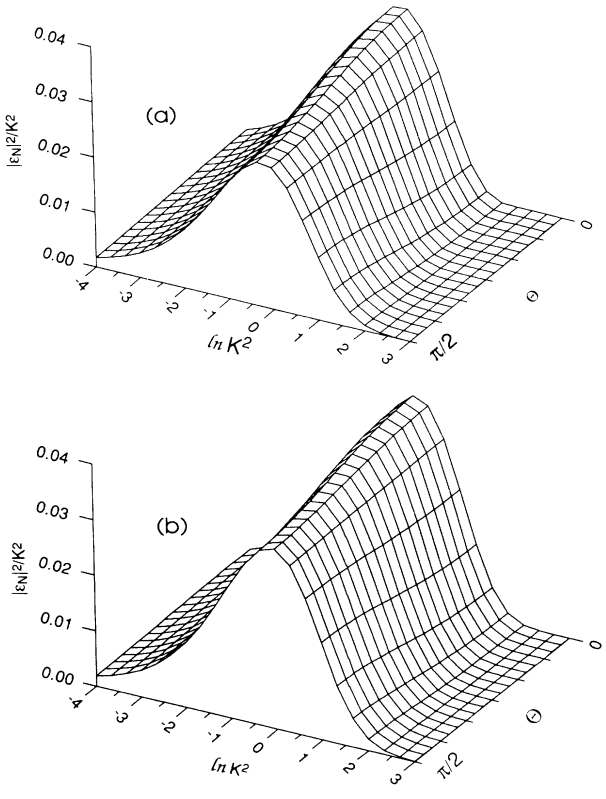

FIG. 7. (a) The exact $1s\sigma$-$2s\sigma$ scattering probability at $R=2$ a.u. (b) The same as Fig. 5 for the $2s\sigma$ final state.

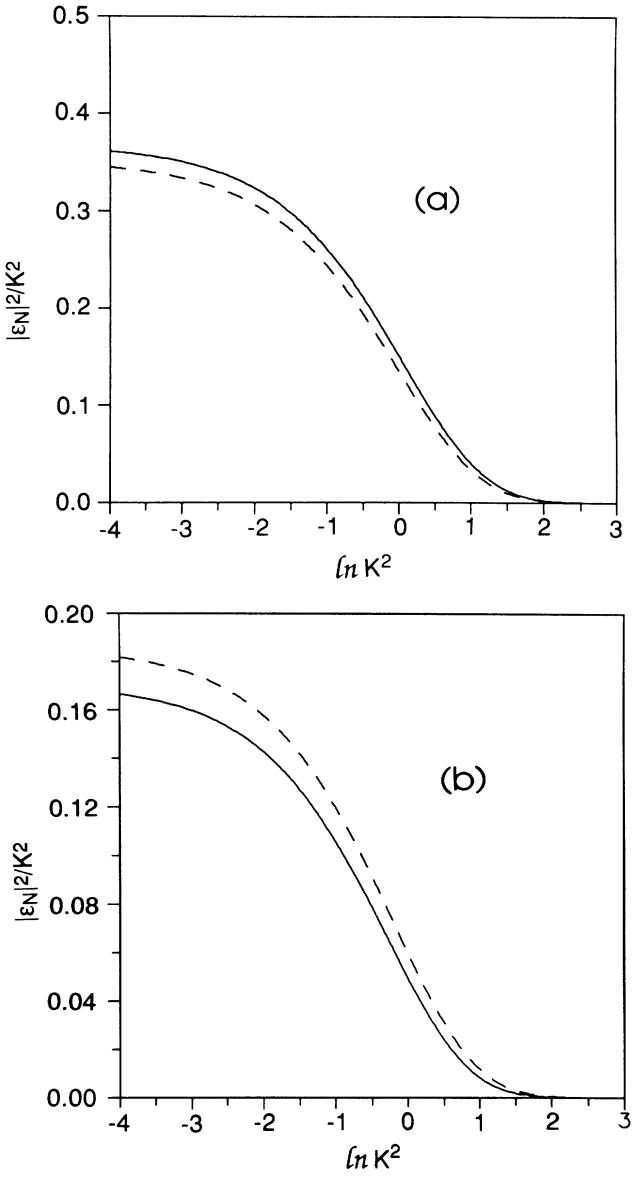

FIG. 8. The θ-averaged transition probabilities using exact (solid lines) and scaled Coulomb (dashed lines) final states for (a) $1s\sigma$-$2p\sigma$ and (b) $1s\sigma$-$2p\pi$ transitions at $R=2$ a.u.

IV. DISCUSSION

The primary electronic excitation amplitudes leading to the dissociation of H_2^+ in fast collisions can be ap-

proximated by Born matrix elements coupling the ground molecular orbital to scaled atomic orbitals representing the final states. At interproton separations near the minimum of the $1s\sigma$ potential well, this approximation reproduces the dependence of the amplitudes on both the magnitude and direction of the momentum transfer for $2s\sigma$, $2p\sigma$, $2p\pi$, and $3d\sigma$ final states.

The results reported here indicate the degree to which a single spherical wave component of the final state dominates excitation amplitudes in impulsive collisions. Applications to larger neutral diatomic molecules await the use of a more accurate single-center expansion and are left to future investigations. I simply note that few theoretical calculations of molecular generalized oscillator strengths are presently available. The use of quasiatomic orbitals in analyzing the contribution of low-lying molecular states to dissociative cross sections and angular distributions of dissociation fragments, even on the 10% level, would greatly enhance such efforts.

ACKNOWLEDGMENTS

I thank Joseph Macek for several interesting discussions concerning this study. The support and assistance of Anthony Starace are also gratefully acknowledged. This work was supported by the Division of Chemical Sciences, Office of Basic Energy Sciences of the U.S. Department of Energy under Grant No. DE-FG02-88ER13955.

---

*Present address: The Joint Institute for Laboratory Astrophysics, University of Colorado, Boulder, CO 80309.

[1]G. H. Dunn, Phys. Rev. Lett. **8**, 62 (1962).
[2]J. M. Peek, Phys. Rev. **134**, A877 (1964).
[3]M. Kimura, Phys. Rev. A **35**, 4101 (1987).
[4]J. M. Peek, Phys. Rev. **140**, A11 (1965).
[5]For a review, see G. W. McClure and J. M. Peek, *Dissociation in Heavy Particle Collisions* (Wiley-Interscience, New York, 1972), Chap. VII.
[6]M. Inokuti, Rev. Mod. Phys. **43**, 297 (1971).
[7]E. H. Kerner, Phys. Rev. **92**, 1441 (1953).
[8]D. R. Bates, K. Ledsham, and A. L. Stewart, Philos. Trans. R. Soc. London Ser. A **246**, 215 (1953).
[9]See Fig. 7 of Ref. 3.
[10]See, D. H. Jaecks, O. Yenen, M. Natarajan, and D. Mueller, Phys. Rev. Lett. **50**, 825 (1983), and references therein.